

# Chandra Observations of the Faintest Low-Mass X-ray Binaries

Colleen A. Wilson<sup>1</sup>, Sandeep K. Patel<sup>2</sup>, Chryssa Kouveliotou<sup>1,3</sup>

*SD 50 Space Science Research Center, National Space Science and Technology Center, 320 Sparkman Drive, Huntsville, AL 35805*

[colleen.wilson-hodge@nssstc.nasa.gov](mailto:colleen.wilson-hodge@nssstc.nasa.gov)

Peter G. Jonker

*Institute of Astronomy, Cambridge University, Madingley Road, CB30HA, Cambridge, United Kingdom*

Michiel van der Klis

*Astronomical Institute 'Anton Pannekoek', University of Amsterdam and Centre for High-Energy Astrophysics, Kruislaan 403, 1098 SJ Amsterdam, the Netherlands*

Walter H.G Lewin

*Department of Physics and Center for Space Research, Massachusetts Institute of Technology, Cambridge, MA 02138*

Tomaso Belloni

*Osservatorio Astronomico di Brera, Via E. Bianchi 46, 23807 Merate (LC), Italy*

Mariano Mendez

*SRON National Institute for Space Research, Sorbonnelaan 2, 3584 CA Utrecht, The Netherlands*

## ABSTRACT

There exists a group of persistently faint galactic X-ray sources that, based on their location in the galaxy, high  $L_x/L_{\text{opt}}$ , association with X-ray bursts, and absence of low frequency X-ray pulsations, are thought to be low-mass X-ray binaries (LMXBs). We present results from Chandra observations for eight of these systems: 4U 1708–408, 2S 1711–339, KS 1739–304, SLX 1735–269, GRS 1736–297, SLX 1746–331, 1E 1746.7–3224, and 4U 1812–12. Locations for all sources, excluding GRS 1736–297, SLX 1746–331, and KS 1739–304 (which were not detected) were improved to 0.6" error circles (90% confidence). Our observations support earlier findings of transient behavior of GRS 1736–297, KS 1739–304, SLX 1746–331, and 2S 1711–339 (which we detect in one of two observations). Energy spectra for 4U 1708–408, 2S 1711–339, SLX 1735–269, 1E 1746.7–3224, and 4U 1812–12 are hard, with power law indices typically 1.4–2.1, which are consistent with typical faint LMXB spectra.

*Subject headings:* Accretion, Accretion Disks, Stars: Binaries: Close, stars: individual (4U 1708–408, 2S 1711–339, KS 1739–304, SLX 1735–269, GRS 1736–297, SLX 1746–331, 1E 1746.7–3224, 4U 1812–12), X-rays: Stars

## 1. Introduction

Low mass X-ray binaries (LMXBs) are systems in which a low mass ( $< 1 M_{\odot}$ ) star transfers matter to either a low magnetic field (typically  $\sim 10^9$  G) neutron star or a black hole. In both cases plasma flows down to a few stellar radii and produces observable properties in X-rays (spectra and timing). Over the last several years comprehensive studies of these properties have provided crucial information on fundamental properties of compact objects, e.g., the equation of state of neutron stars (see van der Klis 2000 for a review), or general relativistic effects near black hole horizons (see Tanaka & Lewin 1995, Esin et al. 2001). However, there exist several sources whose X-ray properties indicate they may also be LMXBs but whose X-ray emission was so faint that no instruments were sensitive enough to study them until the launch of *Chandra*. This paper describes our *Chandra* observations of eight such objects listed as candidate LMXBs in van Paradijs (1995); the accurate locations we derived with *Chandra* will enable follow up observations in the infrared/optical.

Below we briefly summarize prior observations for each of these objects. Table 1 provides a convenient comparison of the observed fluxes discussed below with our *Chandra* observations.

**4U 1708–40** is a persistent X-ray source that was observed by most of the early X-ray instruments, e.g. *Uhuru*, *OSO-7*, *Ariel V*, and *HEAO-1* (van Paradijs 1995, and references therein). A *ROSAT* source, 1RXS J17141224.8–405034, at R.A.  $17^h12^m24^s.8$ , Decl.  $= -40^{\circ}50'34''.5$  (J2000,  $1-\sigma$  error radius =  $10''$ ), detected in the *ROSAT* all-sky survey, lies in the error box for 4U 1708–40 (Voges et al. 1999). Since 1996, 4U 1708–40 has been a persistent source in the *Rossi X-ray Timing Explorer (RXTE)* All-Sky Monitor (ASM). Its 2–10 keV flux<sup>4</sup> slowly declined from about  $6.2 \times 10^{-10}$  ergs cm $^{-2}$  s $^{-1}$  in 1996–1997 to a minimum of about  $1.0 \times 10^{-10}$  ergs cm $^{-2}$  s $^{-1}$  in mid-1998, followed by a slow rise to about  $8.3 \times 10^{-10}$  ergs

cm $^{-2}$  s $^{-1}$  in mid-2001, and a second slow decline that continued in 2002–2003. At the time of our *Chandra* observations, the 2–10 keV flux level in the *RXTE* ASM was about  $5.2 \times 10^{-10}$  ergs cm $^{-2}$  s $^{-1}$ . Migliari et al. (2003) reported the discovery of X-ray bursts in a *BeppoSAX* observation of 4U 1708–408 in 1999 August. During this observation, the spectrum of the persistent flux (before and after the bursts) was well fitted with an absorbed power-law with a column density  $N_H = (2.93 \pm 0.08) \times 10^{22}$  cm $^{-2}$ , a photon index of  $2.42 \pm 0.02$ , and a Gaussian iron line. The unabsorbed 2–10 keV flux was  $1.2 \times 10^{-10}$  ergs cm $^{-2}$  s $^{-1}$ . In addition, Migliari et al. (2003) also reported results for several *RXTE* observations in 1997 and 2000 along with an additional *BeppoSAX* observation in 2001 during which no bursts were seen; however, steady persistent emission was observed. The energy spectra in these observations required more complicated models, an absorbed power law with photon index  $\sim 2.7$  for an assumed  $N_H = 2.9 \times 10^{22}$  cm $^{-2}$ , and a blackbody component with  $kT \sim 1.3$  keV. The unabsorbed 2–10 keV fluxes were  $7.4 \times 10^{-10}$  ergs cm $^{-2}$  s $^{-1}$  and  $8.9 \times 10^{-10}$  ergs cm $^{-2}$  s $^{-1}$  in the 2000 June 18 *RXTE* and 2001 August *BeppoSAX* observations, respectively.

**2S 1711–339** is an X-ray burster originally detected with *Ariel V* (Carpenter et al. 1977) and more precisely located with *SAS-3* (Greenhill, Thomas, & Duldig 1979). A radio source was detected in the *SAS-3* error circle at R.A.  $= 17^h10^m52^s$ , Decl.  $= -34^{\circ}00'36''$  (B1950, 90% confidence error radius  $2.2'$ ) in 1978 July (Greenhill, Thomas, & Duldig 1979). A *ROSAT* source, RXS J171419.3–34023 (Voges et al. 1999), also lies within the *SAS-3* error circle, but just outside the radio source error circle. More recently, Cornelisse et al. (2002) reported on observations of 2S 1711–339 with *BeppoSAX*, the *RXTE* ASM, and *Chandra*. The *RXTE* ASM detected an X-ray outburst of 2S 1711–339 from 1998 July until 1999 May at a 2–10 keV flux level of  $8.2 \times 10^{-10}$  ergs cm $^{-2}$  s $^{-1}$ . During that time period, *BeppoSAX* detected 10 short X-ray bursts, with a persistent flux level (before and after the bursts) of  $6.3 \times 10^{-10}$  ergs cm $^{-2}$  s $^{-1}$  (2–28 keV). The persistent emission was fitted with a cutoff power-law with photon index 0.7, high energy cutoff 2.8 keV,

<sup>1</sup>NASA's Marshall Space Flight Center

<sup>2</sup>National Academy of Sciences NRC Fellow

<sup>3</sup>Universities Space Research Association

<sup>4</sup>Throughout this paper we use the conversion factors 1 mCrab = 0.75 ASM ct/s =  $2.08 \times 10^{-11}$  ergs cm $^{-2}$  s $^{-1}$  (2–10 keV).

and an assumed  $N_H$  of  $1.5 \times 10^{22} \text{ cm}^{-2}$ , derived from *BeppoSAX* Narrow Field Instrument (NFI) observations on 2000 February 29, when the 2-6 keV flux was  $2.4 \times 10^{-11} \text{ ergs cm}^{-2} \text{ s}^{-1}$ . On 2000 March 22, one burst was detected with *BeppoSAX*, but the 3- $\sigma$  upper limit on the persistent flux (before and after the burst) was  $\lesssim 7 \times 10^{-11} \text{ ergs cm}^{-2} \text{ s}^{-1}$  (2-28 keV). The *Chandra* observation, also described in this paper, on 2000 June 9, yielded a location of R.A. =  $17^h 14^m 19.8^s$ , Decl. =  $-34^\circ 02' 47''$  (J2000, 90% confidence error radius 1''), which was consistent with the Wide Field Camera (Cornelisse et al. 2002), *Ariel V* (Carpenter et al. 1977), and *ROSAT* (Voges et al. 1999) positions. The *Chandra* position, however, lies 0.2' outside the 90% confidence error circle of the radio source.

**SLX 1735–269** is an X-ray burster first reported in 1985 from Spacelab-2 X-ray Telescope (XRT) observations (Skinner et al. 1987). It was present in the *Einstein* slew survey 5 years earlier (Elvis et al. 1992). A *ROSAT* source, 1RXS J173817.0–265940, lies within the *Einstein* error circle (Voges et al. 1999). *Granat* Sigma observations showed it to be a persistent hard X-ray source (Goldwurm et al. 1996). Type I X-ray bursts were discovered with the *BeppoSAX* Wide Field Camera (Bazzano et al. 1997, WFC). *ASCA* observations showed the 0.6-10 keV spectrum to be well fitted with a power-law with photon index 2.15 and  $N_H \sim (1.4 - 1.5) \times 10^{22} \text{ cm}^{-2}$  (David et al. 1997), which was consistent with the values derived from *ROSAT* and *Granat* ART-P observations (Pavilinsky, Grebenev, & Sunyaev 1994; Grebenev, Pavilinsky, & Sunyaev 1996). Using *RXTE* observations from 1997 February-May, Wijsnands & van der Klis (1999) showed that the power spectrum was characterized by a strong band limited noise component which was approximately flat below a break frequency of 0.1-2.3 Hz. Above the break frequency the power spectrum declines as a power law of index 0.9. At the highest count rates, a broad bump was observed around 0.9 Hz. The strength of the noise (2-60 keV, integrated over 0.01-100 Hz) was  $\sim 24\%$  and  $\sim 17\%$  rms in the high and low count rate data, respectively. Fits to energy spectra yielded power law indices of 2.2 and 2.4 (with an assumed  $N_H$  of  $1.47 \times 10^{22} \text{ cm}^{-2}$ ) and 3-25 keV fluxes of  $3.8 \times 10^{-10}$

$\text{ergs cm}^{-2} \text{ s}^{-1}$  and  $2.8 \times 10^{-10} \text{ ergs cm}^{-2} \text{ s}^{-1}$ , respectively. Power spectra, from extended *RXTE* observations in 1997 October (Barret et al. 2000) at a 1-20 keV flux level of  $\sim 7.2 \times 10^{-10} \text{ ergs cm}^{-2} \text{ s}^{-1}$ , had a noise strength of 27.6% (2-40 keV, integrated over 0.005-300 Hz) and a break frequency of 0.08-0.15 Hz that appeared to increase with intensity. Belloni, Psaltis, & van der Klis (2002) fitted this power spectrum with a four-Lorentzian model and found a remarkable resemblance to observations of the low-luminosity X-ray burster 1E 1724–3045. SLX 1735–269 has been detected as a persistent source with the *RXTE* ASM since 1996 at an average 2-10 keV flux level of about  $3.1 \times 10^{-10} \text{ ergs cm}^{-2} \text{ s}^{-1}$ .

**GRS 1736–297** was discovered with the *Granat* ART-P telescope in September 1990 and was subsequently observed about a month later (Pavilinsky, Grebenev, & Sunyaev 1992) at a similar flux level. Its spectrum was characterized by a power law with photon index of 1.8 and a 3-12 keV flux of  $6 \times 10^{-11} \text{ ergs cm}^{-2} \text{ s}^{-1}$ . Motch et al. (1998) identified RX J1739.5–2942 with GRS 1736–297, since it lies well within the 90% confidence 90'' radius *Granat* error circle (Pavilinsky, Grebenev, & Sunyaev 1994). Further, Motch et al. (1998) identified a Be star in the *ROSAT* error circle, suggesting that, although GRS 1736–297 has been previously classified as a candidate LMXB (van Paradijs 1995), it may instead be a transient Be/X-ray binary system.

**KS 1739–304** is a transient X-ray source discovered with *MIR/KVANT* in 1989 at a 2-30 keV flux level of about 9 mCrab and located to within a 1.6' error circle (Sunyaev et al. 1991; Cherepashchuk et al. 1994). Subsequent observations with *Granat* ART-P in Autumn 1990 did not detect the source, with a 3- $\sigma$  upper limit of 2 mCrab (8-20 keV) (Pavilinsky, Grebenev, & Sunyaev 1994). Very little is known about this object.

**SLX 1746–331** was discovered with the Spacelab-2 XRT in 1985 August (Skinner et al. 1990). It had a very soft spectrum, best fitted with a thermal Bremsstrahlung with  $kT = 1.5 \text{ keV}$  and a 2-10 keV flux of  $6.35 \times 10^{-10} \text{ ergs cm}^{-2} \text{ s}^{-1}$ . Based on the very soft spectrum, Skinner et al. (1990) suggested

SLX 1746–331 as a potential black hole candidate. The position of SLX 1746–331 fell between fields in the *Einstein* galactic plane survey of Hertz & Grindlay (1984) and it was not detected in the *EXOSAT* galactic plane survey (Warwick et al. 1988). During the *ROSAT* survey observation in 1990 September, 1RXS J174948.4–331215, which lies in the error circle of SLX 1746–331, was detected in outburst, but it was not detected in subsequent *ROSAT* High Resolution Imager (HRI) observations in 1994 October (Motch et al. 1998). Hence the *EXOSAT* and *ROSAT* non-detections suggest this object is a transient system.

**1E 1746.7–3224** was discovered during the *Einstein* galactic plane survey (Hertz & Grindlay 1984), at a 2–10 keV flux level of  $3 \times 10^{-12}$  ergs cm $^{-2}$  s $^{-1}$ . Spacelab-2 XRT observations in 1985 August gave an upper limit on the 2–10 keV flux of  $\lesssim 4 \times 10^{-11}$  ergs cm $^{-2}$  s $^{-1}$  (Skinner et al. 1990). During the *ROSAT* all-sky survey, 1RXS J175003.8–322622 was detected in the *Einstein* error circle of 1E 1746.7–3224 (Voges et al. 1999). Very little is known about this object.

**4U 1812–12** was first detected with *Uhuru* (Forman, Jones, & Tananbaum 1976; Forman et al. 1978) and was later observed by several satellites, including *OSO-7*, *Ariel V*, *HEAO-1*, and *EXOSAT* with a typical 2–10 keV flux of  $\sim 4 \times 10^{-10}$  ergs cm $^{-2}$  s $^{-1}$  (van Paradijs 1995, and references therein). 4U 1812–12 was detected in the *ROSAT* All-Sky Survey as a bright source denoted 1RXS J181506.1–120545 (Voges et al. 1999). X-ray bursts were first detected from this source in 1982 with Hakicho (Murakami et al. 1983) and later with *BeppoSAX* (Cocchi et al. 2000). 4U 1812–12 is classified as an atoll source and shows band limited noise with a break frequency of 0.095 Hz and a QPO at 0.85 Hz (Wijnands & van der Klis 1999). 4U 1812–12 has been detected as a persistent source with the *RXTE* ASM since 1996 at an average 2–10 keV flux level of about  $3.7 \times 10^{-10}$  ergs cm $^{-2}$  s $^{-1}$ . Recent observations in 2000 April with *RXTE* and *BeppoSAX* show 4U 1812–12 in a hard state with a hard tail extending above 100 keV. The power spectrum was characterized by a  $\sim 0.7$  Hz QPO and three broad noise components, extending above  $\sim 200$  Hz (Barret, Olive, & Oosterbroek 2003).

## 2. Observations and Results

Each of the eight objects was observed using the Advanced CCD Imaging Spectrometer (ACIS) on the *Chandra* X-ray observatory. Table 2 lists the details of the observations. For some sources, data were collected in two different observing modes, timed exposure (TE) mode and continuous clocking (CC) mode. Data obtained in TE mode allow for two-dimensional imaging. Accurate spectroscopy of bright targets, however, is limited due to pulse pile-up. Timing studies are limited by the total number of photons collected and the 3.24 s time resolution. In CC mode, the amount of pile-up is negligible owing to the 2.85 ms time resolution, allowing for accurate spectroscopy and timing. Unfortunately only one of the sources, SLX 1735–269, was detected in CC mode.

The best known location for each object was positioned on the nominal target position of ACIS-S3, a back illuminated CCD on the spectroscopic array (ACIS-S) with good charge transfer efficiency and spectral resolution, with the exception of the CC mode observation of SLX 1735–269 which fell on ACIS-S2, a front illuminated CCD on the spectroscopic array (ACIS-S). Standard processing was performed by the *Chandra* data center. The data were filtered to exclude events with grades 1, 5, 7, hot pixels, bad columns, and events on CCD node boundaries. Analysis in this paper was done using *Chandra* Interactive Analysis of Observations (CIAO)<sup>5</sup> version 2.2.1 and *Chandra* Calibration Database (CALDB)<sup>6</sup> version 2.10. For piled-up sources, the tool *acis\_detect\_afterglow* in the standard processing pipeline can reject valid source photons in addition to afterglow photons resulting from residual charge from cosmic ray events in the CCD pixels. We examined the spatial distribution of afterglow events for each observation using methods described in the CIAO documentation<sup>7</sup>. For TE mode observations of 2S 1711–339 and 1E 1746.7–3224 we found that  $\gtrsim 5\%$  of events consistent with the point source had been rejected; hence we reprocessed the data to retain the afterglow flagged events. For all other observations,  $< 1\%$  of events were rejected, so the standard processing was retained.

<sup>5</sup><http://cxc.harvard.edu/ciao/>

<sup>6</sup><http://cxc.harvard.edu/caldb/index.html>

<sup>7</sup><http://asc.harvard.edu/ciao/threads/acisdetectafterglow/>

## 2.1. Source Locations

Using TE mode data, we extracted source locations for each of the detected sources. These locations are listed in Table 3. Sources were located by one of two methods: (1) 2S 1711-339 and 1E 1746.7-3224 were located using the CIAO tool *wavdetect*. The latter source was observed twice in TE mode and locations from both observations were consistent. (2) 4U 1708-40, SLX 1735-269, and 4U 1812-12 were brighter and suffered from considerable pile-up of photons in the image core, resulting in a source that looked ring shaped with a hole in the center. The CIAO Detect tools were inadequate to provide a good location of the centroid, therefore we modeled the data using a Gaussian function multiplied by a hyperbolic tangent in radius, scaled to approach zero at  $r = 0.0$  (Hulleman et al. 2001). The uncertainty of these locations is limited by systematic effects to a circle with  $\sim 0.6''$  radius (Aldcroft et al. 2000). No other known sources were found in the images, hence we were unable to use astrometry to further improve the locations.

## 2.2. Detection Upper Limits

Three objects, GRS 1736-297, SLX 1746-331, and KS 1739-304 went undetected in all observations. To derive upper limits for these sources, we used the CIAO tool *dmextract* to extract count rates for a  $6''$  radius source region and a background annulus (inner radius =  $6''$ , outer radius =  $30''$ ) centered on the best known position. The 99% confidence upper limits were count rates of  $4.9 \times 10^{-3}$  cts s $^{-1}$ ,  $3.7 \times 10^{-3}$  cts s $^{-1}$ , and  $6.2 \times 10^{-3}$  cts s $^{-1}$  (total counts = 6.0 cts, 5.8 cts, and 4.6 cts) for GRS 1736-297, SLX 1746-331, and KS 1739-304, respectively. Using WebPimms<sup>8</sup>, we estimated an upper limit 1-10 keV absorbed flux of  $7.5 \times 10^{-14}$  ergs cm $^{-2}$  s $^{-1}$  for GRS 1736-297, assuming  $N_H = 1.1 \times 10^{22}$  cm $^{-2}$ , derived using Colden<sup>9</sup>, a web tool based on Dickey & Lockman (1990), and a power law photon index = 1.8 (Pavilinsky, Grebenev, & Sunyaev 1992). Similarly, for SLX 1746-331, we estimated an upper limit 1-10 keV absorbed flux of  $2.0 \times 10^{-14}$  ergs cm $^{-2}$  s $^{-1}$ , assuming  $N_H = 0.4 \times 10^{22}$  cm $^{-2}$ , using Colden, and a thermal Bremsstrahlung spectrum

with  $kT = 1.5$  keV (Skinner et al. 1990). For KS 1739-304, we estimated an upper limit 1-10 keV absorbed flux of  $1.2 \times 10^{-13}$  ergs cm $^{-2}$  s $^{-1}$ , assuming  $N_H = 1.4 \times 10^{22}$  cm $^{-2}$ , using Colden, and a power law photon index = 1.5. A fourth object, 2S 1711-339, that was detected in a TE mode observation in 2000, went undetected in the 2002 CC mode observation. To derive an upper limit for it, we again used *dmextract*, with a  $6''$  radius source region and a background annulus (inner radius =  $6''$ , outer radius =  $30''$ ) centered on the *Chandra* position (shifted to correspond to the 1-dimensional CC mode image) from the 2000 observation, to obtain 99% confidence upper limits of  $6.5 \times 10^{-3}$  cts s $^{-1}$  or a total 30.3 counts for the observation. Using WebPimms with our spectral parameters from the 2000 observation Table 4, we estimate a 1-10 keV upper limit absorbed flux of  $1 \times 10^{-13}$  ergs cm $^{-2}$  s $^{-1}$ , a factor of more than 100 fainter than in the 2000 observation. In the 5 May 2002 observation of KS 1739-304, an object was present at R.A. =  $17^h42^m41^s.07$ , Decl. =  $-30^\circ22'39.3''$ , approximately  $8.2'$  from the expected location of KS 1739-304. We measured a total of approximately 45 counts from this object in the 745 s observation. Given its large separation from KS 1739-304, and the fact that it is well outside the  $1.6'$  radius *MIR/KVANT* error circle (Sunyaev et al. 1991), the two objects are most likely unrelated.

## 2.3. Energy Spectra

Energy spectra were difficult to study for most of these sources because in all but one of the observations where a source was detected, we had only imaging (TE) mode data and pile-up was a problem. For these sources we used two approaches to extract and fit the energy spectra: (1) direct extraction from the TE mode data, fitting the data using the pile-up model and (2) extraction of trailed image spectra. To directly extract spectra and associated response files for each source, we used a source region consisting of a  $6''$  radius circle and a background region consisting of an annulus with inner and outer radii of  $6''$  and  $30''$ , respectively, in the CIAO tool *psextract*. These spectra were then fitted using XSPEC 11.2. For all sources, we fitted data for energies from 0.3-10.0 keV using an absorbed power law model with pile-up (phabs\*powerlaw\*pile-up). For most sources

<sup>8</sup><http://heasarc.gsfc.nasa.gov/Tools/w3pimms.html>

<sup>9</sup><http://asc.harvard.edu/toolkit/colden.jsp>

we found that the PSF fraction treated for pile-up (parameter 5) in the pile-up model, needed to be reduced from its default value of 0.95 to 0.85 to allow the grade morphing parameter (parameter 4) to not be pegged at 1.0 and to allow the model to fit the data at higher energies. For some sources, the pile-up model had no effect on the spectral fits, even though the source was obviously piled-up; hence we used trailed images to characterize those spectra. Results of our fits with the pile-up model are listed in Table 4. Figure 1 shows examples of spectra before and after the pile-up model is applied.

Trailed images were extracted using the CIAO tool *acisreadcorr*. During each row transfer, the detector is exposed to the source for  $40\mu\text{s}$ , but the photons are recorded in the wrong Y position, resulting in a streak along the x-axis. We calculated the total transfer streak exposure time using the following expression

$$t_{\text{trail}}^{\text{exposure}} = t_1 * (1024 * f_{\text{sub}} - dy) * t_{\text{exposure}} / t_2 \quad (1)$$

where  $t_1 = 40\mu\text{s}$ , the time to transfer charge from one row to the next; 1024 is the number of pixels in a row;  $f_{\text{sub}} = 1/4$  is the subarray fraction,  $dy = 50$  is the number of pixels excluded near the source;  $t_{\text{exposure}}$  is the total exposure time in seconds; and  $t_2 = 0.841040$  s, the time for one readout of the subarray. Spectra were extracted using the CIAO tool *psextract* with the source region defined as two boxes along the y-axis, each 6 pixels wide in the x-direction. The two boxes included the entire y-axis, except a region  $\pm 25$  pixels from the y-coordinate of the piled-up source. The EXPOSURE and BACKSCAL keywords in the spectra were corrected for using the results of the CIAO tool *acisreadcorr* and the calculation above. The resulting exposure times and total counts measured from the source in each trailed image are listed in Table 5.

For five of the observations, trailed image spectra could be extracted. We grouped the source spectra into bins containing 15 counts. Then these spectra were fitted in XSPEC 11.2 with an absorbed power-law model (phabs\*powerlaw). For two of the sources, 2S 1711–339 and 1E 1746.7–3224, very few counts remained in the trailed image spectra. The results of fitting trailed image spectra are listed in Table 4 and examples are shown in Figure 2.

For one of the sources, SLX 1735–269, energy spectra were extracted from CC mode data taken on 2000 April 4. A source region consisting of a  $6''$  radius circle and a background region consisting of an annulus with inner and outer radii of  $6''$  and  $30''$ , respectively, was used in the CIAO tool *psextract* to extract source and background spectra for the CC mode data and to create associated detector response files. We then grouped the data in the source spectrum so that each bin contained 25 counts. This observation fell on the ACIS-S2 chip, a front illuminated chip, so the low-energy response was reduced. In XSPEC<sup>10</sup> 11.2 (Arnaud 1996), we fitted data for energies of 1.0–1.8 keV and 2.2–9.0 keV with an absorbed power-law model (phabs\*powerlaw). Fit results are listed in Table 4 and are shown in Figure 3.

The CC mode observations of SLX 1735–269 resulted in the largest number of source counts of any of our sources. Hence we used these observations to investigate if more complicated spectral models are warranted. For example, Migliari et al. (2003) reported an iron line with energy  $6.5 \pm 0.1$  keV, fixed width 0.9 keV, and equivalent width 344 eV in addition to an absorbed power-law in observations of 4U 1708–408. To search for evidence of a similar line in SLX 1735–269, we included a Gaussian with a fixed centroid at 6.5 keV and fixed width of 0.9 keV. Our fit resulted in a 3-sigma upper limit on the equivalent width of 975 eV, indicating that we had insufficient statistics to detect such a line.

Next, since a soft thermal component has been observed in several LMXBs, we fitted a blackbody in addition to the absorbed power-law. The fit gave  $\chi^2 = 278.2$  with 253 degrees of freedom. An F-test comparing this fit to the absorbed power law had a value of 6.02 and a probability of  $2.8 \times 10^{-3}$ , suggesting that a softer component may be present. The resulting fit parameters were:  $N_{\text{H}} = (1.3 \pm 0.1) \times 10^{22} \text{ cm}^{-2}$ , blackbody temperature  $kT = 0.56 \pm 0.03$  keV, blackbody normalization  $(R_{\text{bb}}/d_{10 \text{ kpc}})^2 = 71 \pm 15$ , power law index =  $1.4 \pm 0.2$ , and power law normalization =  $(2.5 \pm 1.1) \times 10^{-2}$  photons  $\text{keV}^{-1} \text{ cm}^{-2} \text{ s}^{-1}$  at 1 keV. Since this observation with the largest number of source counts resulted in only a suggestion of a softer component, we concluded that we had insufficient

---

<sup>10</sup><http://heasarc.gsfc.nasa.gov/docs/software/lheasoft/xanadu/xspec/index.html>

statistics to distinguish spectral models in the rest of our observations, which had significantly fewer source counts.

## 2.4. Timing

Previous *RXTE* observations of SLX 1735–269 with 3-25 keV fluxes  $\gtrsim 3.8 \times 10^{-10}$  ergs cm $^{-2}$  s $^{-1}$  show band limited noise levels with fractional amplitudes of 24-28% and break frequencies of 0.1-0.2 Hz (Wijnands & van der Klis 1999; Barret et al. 2000; Belloni, Psaltis, & van der Klis 2002) and a QPO near 0.9 Hz with a fractional rms of  $\sim 5\%$  and FWHM = 0.3-0.8 Hz. Wijnands & van der Klis (1999) also reported a very different power spectrum from “low count rate” 1997 *RXTE* observations of SLX 1735–269 with 3-25 keV fluxes  $\lesssim 2.8 \times 10^{-10}$  ergs cm $^{-2}$  s $^{-1}$ , that had a break frequency of 2.3 Hz and a fractional rms of 17%. Barret, Olive, & Oosterbroek (2003) fitted *BeppoSAX* power spectra for 4U 1812–12 with a 4 Lorentzian model after Belloni, Psaltis, & van der Klis (2002). The low-frequency Lorentzian, fitting the low-frequency end of the band limited noise, had a fractional amplitude of 9.8% rms and a break frequency of 0.15 Hz. A low-frequency QPO was also detected with *BeppoSAX* at 0.73 Hz with a fractional amplitude of 3.9% rms.

We computed the sensitivity of our Chandra observations to features in the power spectrum using

$$r = (2N_\sigma)^{1/2} \frac{(S+B)^{1/2}}{S} \left( \frac{\Delta\nu}{T} \right)^{1/4} \quad (2)$$

where  $r$  is the fractional root-mean-squared (rms) of the signal;  $N_\sigma$  is the significance of the expected detection;  $S + B$  is the total observed count rate;  $S$  is the source count rate;  $\Delta\nu$  is the full-width half-max (FWHM) of the signal, which is approximately equal to twice the break frequency obtained with a broken power law model for band limited noise (see Belloni, Psaltis, & van der Klis 2002); and  $T$  is the exposure time. For TE-mode observations of SLX 1735–269, 4U 1708–408, 2S 1711–339, 4U 1812–12, and the 2000 Aug 30 observation of 1E 1746.7–3224,  $S + B = 0.2\text{--}0.7$  cts s $^{-1}$ ,  $S = 0.2\text{--}0.7$  cts s $^{-1}$ , and  $T = 950\text{--}6800$  s, resulting in 3- $\sigma$  sensitivities of 30-50% rms for features with  $\Delta\nu = 0.3$  Hz. The 2002 July 16 observation of 1E 1746.7–3224 was longer, with  $T = 8500$  s, and had slightly higher count rates of  $S + B = 1.2$

cts s $^{-1}$  and  $S = 1.2$  cts s $^{-1}$ , resulting in a 3- $\sigma$  sensitivity of 23% rms. Our *Chandra* TE mode observations were not sensitive enough to detect broadband features at previously detected levels. However, the CC mode observation of SLX 1735–269, with  $S + B = 10.3$  cts s $^{-1}$ ,  $S = 10.2$  cts s $^{-1}$ , and  $T = 1400$  s, had a much better 3- $\sigma$  sensitivity of 9.3% rms for  $\Delta\nu = 0.3$  Hz. Hence band limited noise at levels observed in the brighter state of SLX 1735–269 (Wijnands & van der Klis 1999; Barret et al. 2000; Belloni, Psaltis, & van der Klis 2002) should have been detectable in the CC mode observations; however, the observed QPO was not detectable. We estimated a 3- $\sigma$  sensitivity of 18% rms for  $\Delta\nu = 4.6$  Hz, corresponding to the fainter state observed by Wijnands & van der Klis (1999), for our CC mode observation of SLX 1735–269; hence we were unable to confirm this state with our *Chandra* observations.

For the CC mode observation of SLX 1735–269, we created a light curve using CIAO tools<sup>11</sup> that account for the fact that event times recorded in CC mode data were the times the events were read, not the times when the charge was deposited on the detector (Zavlin et al. 2000). We generated a power spectrum for the energy range 0.3-10 keV from the 2.85 ms CC mode light curve. No obvious variability was present in either the light curve or the power spectrum. Integrating from 0.01-1 Hz, we estimated a noise strength of  $\sim 10\%$  rms for this observation; since this noise level was near our detection threshold, we cannot easily confirm that this was entirely source related. However, the lack of strong band limited noise at levels  $> 20\%$  rms, combined with our 1-10 keV flux measurement of  $1.9 \times 10^{-10}$  ergs cm $^{-2}$  s $^{-1}$  suggests that SLX 1735–269 was most likely in a state similar to the “lowest count rate” state reported in Wijnands & van der Klis (1999).

## 2.5. UKIRT Images

We obtained images of SLX 1735–269, 1E 1746.7–3224, and 4U 1812–12 using the United Kingdom Infrared Telescope (UKIRT) to search for near-infrared counterparts. For SLX 1735–269, the seeing was approximately 0.7'', the airmass was 1.46, the upper limit on the presence of a star in the *Chandra* error circle was  $J > 19.4$ . The as-

---

<sup>11</sup><http://asc.harvard.edu/ciao/threads/aciscctoa/>

trometric solution was performed using five stars from the 2Mass in J catalog. The fit was good with an rms of  $0.26''$ . The astrometric accuracy of the 2Mass Catalogue is  $< 0.2''$ . For 1E 1746.7–3224 the seeing was approximately  $0.6''$ , the airmass was 1.64, and the upper limit for a source in the *Chandra* error circle was  $J > 19.6$ . The astrometric solution was performed using eight stars from the 2Mass in J catalog. The fit was good with an rms of  $0.23''$ . There was no 2Mass image available for 4U 1812–12; hence, the astrometric solution of the UKIRT image of the field containing 4U 1812–12 (seeing  $\sim 0.6''$ , airmass 1.18) was obtained by identifying four USNO-A1.0 stars in an optical Digital Sky Survey (DSS) image with a near infrared star. However, with an rms of  $0.8''$  the astrometric solution was poor. A star appears to be present near the error circle, but its J band magnitude is difficult to assess since we have no J band magnitudes for other stars in the field for comparison.

### 3. Discussion

Using *Chandra* we observed eight faint, little studied likely LMXBs. Of the eight systems, we detected five in at least one observation: 4U 1708–408, 2S 1711–339, SLX 1735–269, 1E 1746.7–3224, and 4U 1812–12. The *Chandra* observations reported in this paper resulted in precise locations for all five of these objects, allowing for future deep optical and infrared observations. UKIRT images of SLX 1735–269, 1E 1746.7–3224, and 4U 1812–12 did not reveal counterparts in the J band. Energy spectra for these five systems were generally consistent with hard power laws (with photon index 1.5–2) typical for faint LMXBs (van der Klis 1994; van Paradijs & van der Klis 1994; Barret, McClintock, & Grindlay 1996, and references therein). Absorbed fluxes (1–10 keV) for the detected sources ranged from  $(2.1 - 89) \times 10^{-11}$  ergs  $\text{cm}^{-2} \text{s}^{-1}$ . The relatively narrow range of power law indices and observed fluxes suggest that all five of the detected systems may be in a similar state.

Energy spectra and fluxes for 4U 1708–408, SLX 1735–269, and 4U 1812–12 were consistent with previous measurements in similar energy bands, supporting earlier findings that these systems are persistent. We observed SLX 1735–269

at a 1–10 keV flux level of  $2 \times 10^{-10}$  ergs  $\text{cm}^{-2} \text{s}^{-1}$  in both observations. This combined with the lack of detection of strong band limited noise in the CC mode observation suggests that SLX 1735–269 was in a similar state to the “low count rate” state reported in Wijnands & van der Klis (1999). The energy spectrum and flux measured using the pile-up model with *Chandra* on 2000 June 9 for 2S 1711–339 were consistent with that measured with the *BeppoSAX* NFI on 2000 Feb 29 and with *BeppoSAX* WFC upper limits on 2000 March 22, suggesting that we were observing either an extended tail of the bright 1998–1999 outburst observed with *BeppoSAX* and *RXTE* or a faint outburst. An estimate of the 2–6 keV flux reported in Cornelisse et al. (2002) from the 2000 June 9 *Chandra* observation was a factor of  $\gtrsim 10$  fainter than the flux we measured with *Chandra* for the same observation. We believe that Cornelisse et al. (2002) did not properly account for the effects of pulse pile-up. In our second *Chandra* observation of 2S 1711–339, in 2002 March, it had faded below detectability in CC mode. 1E 1746.7–3224, the least studied of our five detected sources, and the only one of the five not to have previously shown X-ray bursts, was observed with *Chandra* at absorbed 1–10 keV fluxes of  $2.1 \times 10^{-11}$  ergs  $\text{cm}^{-2} \text{s}^{-1}$  and  $(3.2 - 3.3) \times 10^{-11}$  ergs  $\text{cm}^{-2} \text{s}^{-1}$  in 2000 and 2002, respectively. In the *ROSAT* all-sky survey (Voges et al. 1999), 1E 1746.7–3224 was measured at a count rate of 0.08 counts  $\text{s}^{-1}$  in the Position Sensitive Proportional Counter (PSPC). This corresponds to an absorbed 1–10 keV flux of  $(2 - 3) \times 10^{-11}$  ergs  $\text{cm}^{-2} \text{s}^{-1}$ , if the spectral shape we measured with *Chandra* is assumed. These fluxes are a factor of  $\sim 10$  higher than that observed in the *Einstein* galactic plane survey (Hertz & Grindlay 1984). The similarity of the *Chandra* and *ROSAT* fluxes suggests this source is persistent, and the *Einstein* measurement suggests that it, like most persistent sources, is also variable. The three undetected systems, GRS 1736–297, KS 1739–304, and SLX 1746–331, had shown previous transient behavior. These non-detections were not due to positional errors. Upper limits on their fluxes were  $(0.2 - 1.2) \times 10^{-13}$  ergs  $\text{cm}^{-2} \text{s}^{-1}$ , two to three orders of magnitude fainter than our faintest detection. If these sources were located at the galactic center, at a distance of 8 kpc, then these fluxes would correspond to luminosities of

$(2 - 9) \times 10^{32}$  ergs s $^{-1}$ .

The United Kingdom Infrared Telescope is operated by the Joint Astronomy Centre on behalf of the U.K. Particle Physics and Astronomy Research Council, and some of the data reported here were obtained as part of the UKIRT Service Programme. CK and SP are partly supported by SAO grants GO0-1054A and GO2-3046B. WHGL is grateful for support from NASA.

## REFERENCES

Aldcroft, T.L., Karovska, M., Cresitello-Ditmar, M.L., Cameron, R.A., & Markevitch, M.L. 2000, Proc. SPIE, 4012, 650

Arnaud, K.A. 1996, Astronomical Data Analysis Software and Systems V, eds. G. Jacoby & J. Barnes, ASP Conf. Series, 101, 17

Barret, D. et al. 2000, ApJ 533, 329

Barret, D., McClintock, J.E., & Grindlay, J.E. 1996, ApJ, 473, 963

Barret, D., Olive, J.F., & Oosterbroek, T. 2003, A&Ain press, astro-ph/0301130

Bazzano, A. et al. 1997, IAU Circ., 6668, 2

Belloni, T., Psaltis, D., & van der Klis, M. 2002, ApJ, 572, 392

Carpenter, G.F., Eyles, C.J., Skinner, G. K., Wilson, A. M., & Willmore, A.P. 1977, MNRAS, 179, 297

Cherepashchuk, A.M. et al. 1994, A&A, 289, 419

Cocchi, M. et al. 2000, A&A, 357, 527

Cornelisse, R. et al. 2002, A&A, 392, 885

David, P. et al. 1997, A&A, 322, 229

Dickey, J.M & Lockman, F.J. 1990, ARA&A, 28, 215

Elvis, M. et al. 1992, ApJS, 80, 257

Esin, A.A. et al. 2001, ApJ, 555, 483

Forman, W., Jones, C., Tananbaum, H. 1976, ApJ, 206, L29

Forman, W. et al. 1978, ApJS, 38, 357

Goldwurm, A. et al. 1996, A&A, 310, 857

Grebenev, S.A., Pavilinsky, M.N., & Sunyaev, R.A. 1996, in the 2nd INTEGRAL Workshop: The Transparent Universe, ESA SP-382 (Noordwijk:ESA), 183

Greenhill, J.G. Thomas, R.M. & Duldig, M.L. 1979, Nature, 279, 620

Hertz, P. & Grindlay, J.E. 1984, ApJ, 278, 137

Hulleman, F., Tennant, A.F., van Kerkwijk, M.H., Kulkarni, S.R., Kouveliotou, C. & Patel, S.K. 2001, ApJ, 563, L49

Migliari, S. et al. 2003, MNRAS, in press, astro-ph/0303136

Motch, C. et al. 1998, A&AS, 132, 341

Murakami, T. et al. 1983, PASJ, 35, 531

Pavilinsky, M.N., Grebenev, S.A., & Sunyaev, R.A. 1992, SvAL, 18, 88

Pavilinsky, M.N., Grebenev, S.A., & Sunyaev, R.A. 1994, ApJ, 425, 110

Skinner, G. K. et al. 1987, Nature, 330, 544

Skinner, G.K., Foster, A.J., Willmore, A.P., & Eyles, C.J. 1990, MNRAS, 243, 72

Sunyaev, R. et al. 1991, Adv. Space Res., 11(8), 177

Tanaka, Y. & Lewin, W.H.G 1995, in X-ray Binaries, eds. W.H.G. Lewin, J. van Paradijs, & E.P.J. van den Heuvel, (New York: Cambridge University Press), 126

van der Klis, M. 1994, ApJS, 92, 511

van der Klis, M. 2000, Ann. Rev. Astron. Astrophys., 38, 717

van Paradijs, J. 1995, in X-ray Binaries, eds. W.H.G. Lewin, J. van Paradijs, & E.P.J. van den Heuvel, (New York: Cambridge University Press), 536

van Paradijs, J. & van der Klis, M. 1994, A&A, 281, L17

Voges, W. et al. 1999, A&A, 349, 389

Warwick, R.S., Norton, A.J., Turner, M.J.L.,  
Watson, M.G. & Willingdale, R. 1988, MN-  
RAS, 232, 551

Wijnands, R. & van der Klis, M. 1999a, ApJ, 514,  
939

Wijnands, R. & van der Klis, M. 1999b, A&A,  
345, L35

Zavlin, V.E., Pavlov, G.G., Sanwal, D., &  
Trümper, J. 2000, ApJ, 540, L25

TABLE 1  
SUMMARY OF OBSERVED X-RAY FLUXES<sup>a</sup>

| Object         | Date                   | Instrument                            | Energy Range | Flux (ergs cm <sup>-2</sup> s <sup>-1</sup> ) |
|----------------|------------------------|---------------------------------------|--------------|---|
| 4U 1708-40     | 1996-1997              | <i>RXTE</i> ASM                       | 2-10 keV     | $6.2 \times 10^{-10}$                         |
| ...            | mid-1998               | <i>RXTE</i> ASM                       | 2-10 keV     | $1.0 \times 10^{-10}$                         |
| ...            | 1999 August            | <i>BeppoSAX</i>                       | 2-10 keV     | $1.2 \times 10^{-10}$                         |
| ...            | 2000 May 15            | <i>Chandra</i>                        | 1-10 keV     | $8.7 \times 10^{-10}$                         |
| ...            | 2000 Jun 18            | <i>RXTE</i> PCA                       | 2-10 keV     | $7.4 \times 10^{-10}$                         |
| ...            | mid-2001               | <i>RXTE</i> ASM                       | 2-10 keV     | $8.3 \times 10^{-10}$                         |
| ...            | 2001 August            | <i>BeppoSAX</i>                       | 2-10 keV     | $8.9 \times 10^{-10}$                         |
| 2S 1711-339    | 1998 July - 1999 May   | <i>RXTE</i> ASM                       | 2-10 keV     | $8.2 \times 10^{-10}$                         |
| ...            | 1998 July - 1999 May   | <i>BeppoSAX</i> WFC                   | 2-28 keV     | $6.3 \times 10^{-10}$                         |
| ...            | 2000 February 29       | <i>BeppoSAX</i> NFI                   | 2-6 keV      | $2.4 \times 10^{-11}$                         |
| ...            | 2000 March 22          | <i>BeppoSAX</i> WFC                   | 2-28 keV     | $\lesssim 7 \times 10^{-11}$                  |
| ...            | 2000 June 9            | <i>Chandra</i>                        | 1-10 keV     | $4.4 \times 10^{-11}$                         |
| ...            | 2002 March 12          | <i>Chandra</i>                        | 1-10 keV     | $\lesssim 1 \times 10^{-13}$                  |
| SLX 1735-269   | 1996-2003              | <i>RXTE</i> ASM                       | 2-10 keV     | $3.1 \times 10^{-10}$                         |
| ...            | 1997 February-May      | <i>RXTE</i> PCA                       | 3-25 keV     | $(2.8 - 3.8) \times 10^{-10}$                 |
| ...            | 1997 October           | <i>RXTE</i> PCA                       | 1-20 keV     | $7.2 \times 10^{-10}$                         |
| ...            | 2000 April 4           | <i>Chandra</i>                        | 1-10 keV     | $1.9 \times 10^{-10}$                         |
| ...            | 2000 May 23            | <i>Chandra</i>                        | 1-10 keV     | $2.1 \times 10^{-10}$                         |
| GRS 1736-297   | 1990 September-October | <i>Granat</i> ART-P                   | 3-12 keV     | $6 \times 10^{-11}$                           |
| ...            | 2000 May 31            | <i>Chandra</i>                        | 1-10 keV     | $\lesssim 8 \times 10^{-14}$                  |
| KS 1739-304    | 1989                   | <i>MIR/KVANT</i>                      | 2-30 keV     | $2 \times 10^{-10}$                           |
| ...            | 1990                   | <i>Granat</i> ART-P                   | 8-20 keV     | $\lesssim 5 \times 10^{-11}$                  |
| ...            | 2002 May 5             | <i>Chandra</i>                        | 1-10 keV     | $\lesssim 1 \times 10^{-13}$                  |
| SLX 1746-331   | 1985 August            | Spacelab-2 XRT                        | 2-10 keV     | $6.35 \times 10^{-10}$                        |
| ...            | 2000 June 9            | <i>Chandra</i>                        | 1-10 keV     | $\lesssim 2 \times 10^{-14}$                  |
| 1E 1746.7-3224 | 1978-1981              | <i>Einstein</i>                       | 2-10 keV     | $3 \times 10^{-12}$                           |
| ...            | 1985 August            | Spacelab-2 XRT                        | 2-10 keV     | $\lesssim 4 \times 10^{-11}$                  |
| ...            | 1990-1991              | <i>ROSAT</i> PSPC                     | 1-10 keV     | $(2 - 3) \times 10^{-11}$                     |
| ...            | 2000 August 30         | <i>Chandra</i>                        | 1-10 keV     | $2.1 \times 10^{-11}$                         |
| ...            | 2002 July 15-16        | <i>Chandra</i>                        | 1-10 keV     | $(3.2 - 3.3) \times 10^{-11}$                 |
| 4U 1812-12     | ...                    | <i>OSO-7, Ariel V, HEAO-1, EXOSAT</i> | 2-10 keV     | $4 \times 10^{-10}$                           |
| ...            | 1996-2003              | <i>RXTE</i> ASM                       | 2-10 keV     | $3.7 \times 10^{-10}$                         |
| ...            | 2000 June 14           | <i>Chandra</i>                        | 1-10 keV     | $4.4 \times 10^{-10}$                         |

<sup>a</sup>This table is intended as a convenient summary of observed fluxes discussed in the text and is not meant to be a complete record of all observations.

<sup>b</sup>Unabsorbed flux.

TABLE 2  
*Chandra* OBSERVATIONS

| Target Object  | Observation ID | Date           | ACIS-S Mode     | Time Resolution | Exposure Time (ks) | Detected |
|----------------|----------------|----------------|-----------------|-----------------|--------------------|----------|
| 4U 1708–40     | 661            | 2000 May 15    | TE              | 0.841 s         | 1.2                | Y        |
| 2S 1711–339    | 662            | 2000 Jun 9     | TE              | 0.841 s         | 1.0                | Y        |
| ...            | 2695           | 2002 Mar 12    | CC              | 2.85 ms         | 4.7                | N        |
| SLX 1735–269   | 664            | 2000 Apr 4     | CC <sup>a</sup> | 2.85 ms         | 1.4                | Y        |
| ...            | 663            | 2000 May 23    | TE              | 0.841 s         | 1.7                | Y        |
| GRS 1736–297   | 665            | 2000 May 31    | TE              | 0.841 s         | 1.3                | N        |
| ...            | 666            | 2000 Jul 7     | CC              | 2.85 ms         | 12.2               | N        |
| KS 1739–304    | 2696           | 2002 Apr 27    | CC              | 2.85 ms         | 3.4                | N        |
| ...            | 2697           | 2002 May 5     | TE              | 3.24 s          | 0.8                | N        |
| SLX 1746–331   | 667            | 2000 Jun 9     | TE              | 0.841 s         | 1.7                | N        |
| ...            | 668            | 2000 Jul 24    | CC              | 2.85 ms         | 4.1                | N        |
| 1E 1746.7–3224 | 669            | 2000 Aug 30    | TE              | 3.24 s          | 6.8                | Y        |
| ...            | 2698           | 2002 Jul 15–16 | TE              | 0.841 s         | 8.5                | Y        |
| 4U 1812–12     | 670            | 2000 Jun 14    | TE              | 3.24 s          | 1.0                | Y        |

<sup>a</sup>This observation fell on the S2 chip, rather than the standard S3 chip.

TABLE 3  
SOURCE LOCATIONS (J2000).<sup>a</sup>

| Object                      | Right Ascension                                     | Declination  |
|-----------------------------|---|--------------|
| 4U 1708–40                  | 17 <sup>h</sup> 12 <sup>m</sup> 23. <sup>s</sup> 83 | -40°50'34.0" |
| 2S 1711–339                 | 17 <sup>h</sup> 14 <sup>m</sup> 19. <sup>s</sup> 78 | -34°02'47.3" |
| SLX 1735–269                | 17 <sup>h</sup> 38 <sup>m</sup> 17. <sup>s</sup> 12 | -26°59'38.6" |
| 1E 1746.7–3224 <sup>b</sup> | 17 <sup>h</sup> 50 <sup>m</sup> 3. <sup>s</sup> 90  | -32°25'50.4" |
| ...                         | 17 <sup>h</sup> 50 <sup>m</sup> 3. <sup>s</sup> 95  | -32°25'50.1" |
| 4U 1812–12                  | 18 <sup>h</sup> 15 <sup>m</sup> 06. <sup>s</sup> 18 | -12°05'47.1" |

<sup>a</sup>90% confidence error radius  $\simeq 0.6''$  on axis.

<sup>b</sup>2000 Aug 30 observation.

<sup>c</sup>2002 Jul 15–16 observation.

TABLE 4  
SPECTRAL FITTING RESULTS<sup>a</sup>

| Object         | Date           | Type <sup>b</sup> | $N_H$<br>( $10^{22} \text{ cm}^{-2}$ ) | Index           | $\alpha^c$      | $\chi^2/\text{dof}$ | Flux (1-10 keV)<br>$10^{-11} \text{ ergs cm}^{-2} \text{ s}^{-1}$ |
|----------------|----------------|-------------------|--|-----------------|-----------------|---------------------|---|
| 4U 1708-40     | 2000 May 15    | Tr                | $3.3 \pm 0.5$                          | $1.9 \pm 0.3$   | ...             | 14.2/15             | 87  |
| 2S 1711-339    | 2000 Jun 9     | TE                | $1.5 \pm 0.3$                          | $1.9 \pm 0.2$   | $0.64 \pm 0.02$ | 11.8/18             | 4.4   |
| ...            | ...            | Tr                | $0.9 \pm 0.4$                          | $1.9 \pm 0.7$   | ...             | 2.8/2               | 11  |
| ...            | 2002 Mar 12    | CC                | $1.4^d$                                | $1.9^d$         | ...             | ...                 | $\lesssim 0.01^e$   |
| SLX 1735-269   | 2000 Apr 4     | CC                | $1.70 \pm 0.05$                        | $2.07 \pm 0.04$ | ...             | 291.4/255           | 19  |
| ...            | 2000 May 23    | Tr                | $1.8 \pm 0.5$                          | $2.2 \pm 0.6$   | ...             | 13.1/10             | 21  |
| GRS 1736-297   | 2000 May 31    | TE                | $1.1^d$                                | $1.8^d$         | ...             | ...                 | $\lesssim 0.008^e$  |
| KS 1739-304    | 2002 May 5     | TE                | $1.4^d$                                | $1.5^d$         | ...             | ...                 | $\lesssim 0.01^e$   |
| SLX 1746-331   | 2000 Jun 9     | TE                | $0.4^d$                                | $1.5^f$         | ...             | ...                 | $\lesssim 0.002^e$  |
| 1E 1746.7-3224 | 2000 Aug 30    | TE                | $2.0 \pm 0.1$                          | $1.54 \pm 0.06$ | $0.96 \pm 0.02$ | 40.2/44             | 2.1   |
| ...            | 2002 Jul 15-16 | TE                | $1.5 \pm 0.1$                          | $1.1 \pm 0.1$   | $0.51 \pm 0.06$ | 186.1/183           | 3.2   |
| ...            | ...            | Tr                | $1.3 \pm 0.7$                          | $1.2 \pm 0.7$   | ...             | 0.1/1               | 3.3   |
| 4U 1812-12     | 2000 Jun 14    | Tr                | $1.1 \pm 0.2$                          | $1.5 \pm 0.3$   | ...             | 16.4/9              | 44  |

<sup>a</sup>Errors on spectral fitting parameters are  $1\sigma$ .

<sup>b</sup>Tr = Trailed image, TE = Timed exposure mode (with pile-up model), CC = Continuous clocking mode

<sup>c</sup>Pile-up parameter.

<sup>d</sup>Assumed spectral parameter.

<sup>e</sup>99% confidence upper limit from WebPimms.

<sup>f</sup>Thermal Bremsstrahlung spectrum with  $kT = 1.5$  keV assumed.

TABLE 5  
TRAILED IMAGE SPECTRA EXPOSURE AND SOURCE COUNTS

| Object         | Date           | Exposure (s) | Total Source Counts |
|----------------|----------------|--------------|---------------------|
| 4U 1708-40     | 2000 May 15    | 11.2         | 412                 |
| 2S 1711-339    | 2000 Jun 9     | 8.84         | 86                  |
| SLX 1735-269   | 2000 May 23    | 16.0         | 228                 |
| 1E 1746.7-3224 | 2002 Jul 15-16 | 79.4         | 117                 |
| 4U 1812-12     | 2000 Jun 14    | 11.9         | 312                 |

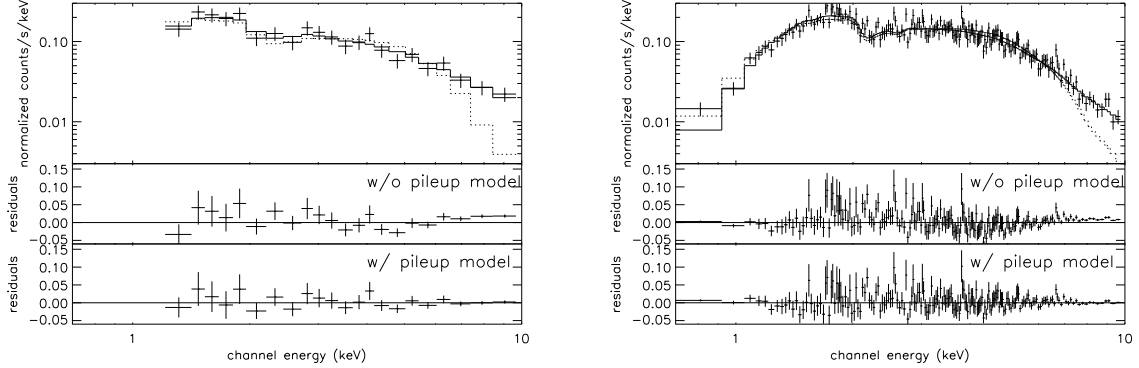


Fig. 1.— Energy spectra extracted from TE mode images, fitted using an absorbed power-law model (dotted line) and a piled-up absorbed power-law (solid line) for 2S 1711–339 (left) and 1E 1746.7–3224 (right).

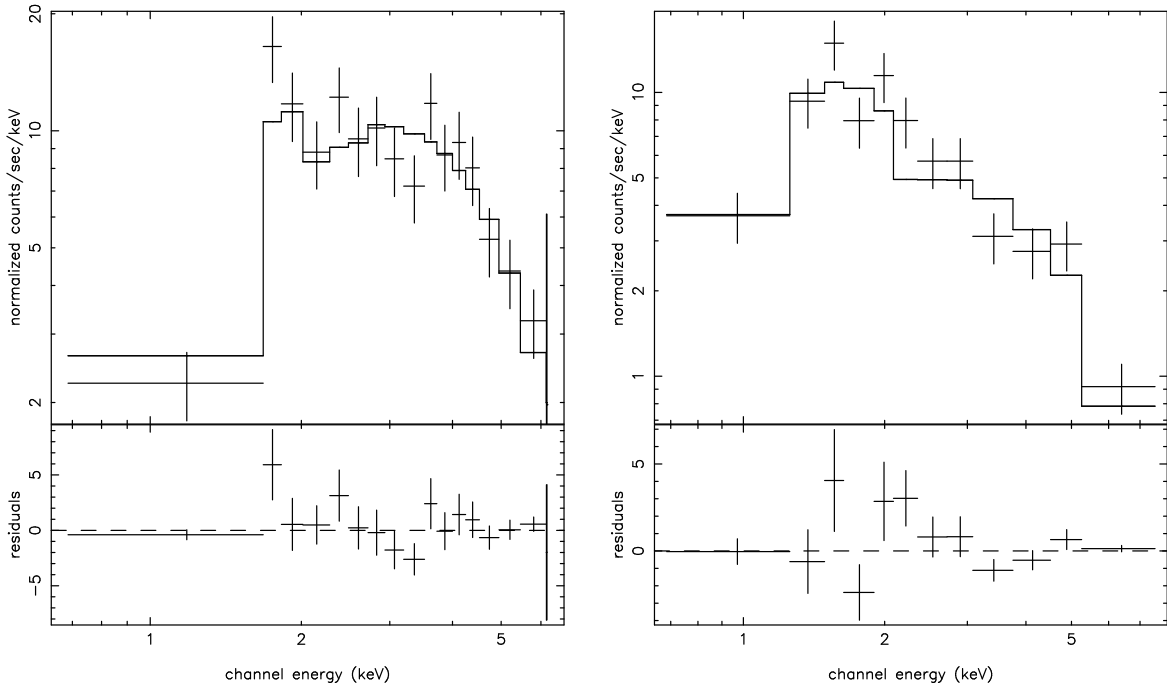


Fig. 2.— Trailedd image spectra for 4U 1708–408 (left) and 4U 1812–12 (right).

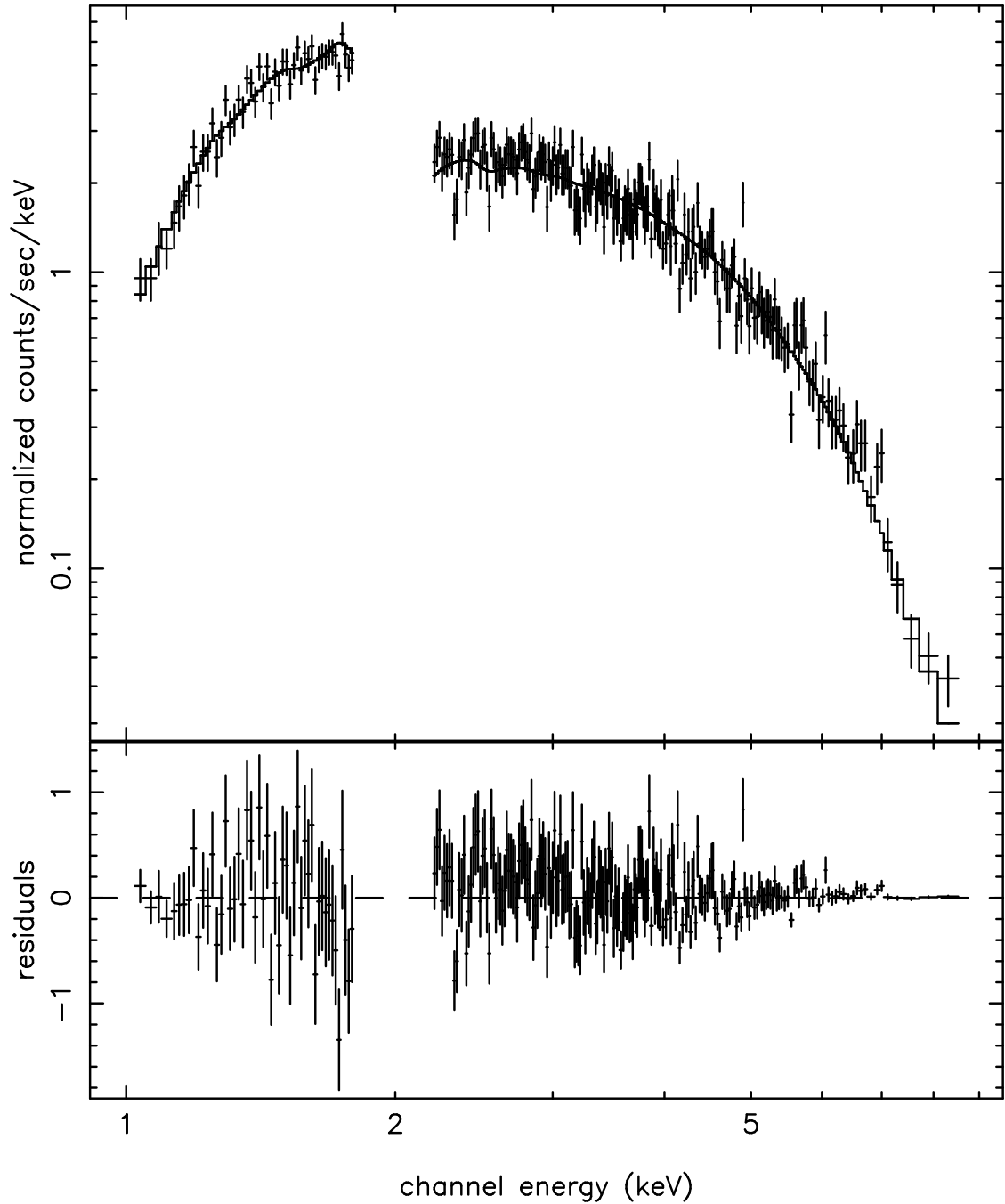


Fig. 3.— Continuous Clocking mode energy spectrum for SLX 1735–269. This observation fell on the S2 chip, a front illuminated CCD.